A Theoretical Study for the Design of a New Ballistic Range

G. Rajesh
School of Mechanical Engineering, Andong National University,
388, Songcheon-dong, Andong, Gyeongbuk 760-749, Korea
J. M. Lee
Angang Plant, Poongsan Co.,
Gyeongju, Gyeongbuk, 780-805, Korea
S. C. Back
Digital Appliance Company, LG Electronics Inc.,
391-2, Ga Eum Jeong-Dong, Changwon City, Gyeong Nam 641-711, Korea
Heuy Dong Kim*
School of Mechanical Engineering, Andong National University,
388, Songcheon-dong, Andong, Gyeongbuk 760-749, Korea

The ballistic range has long been employed in a variety of engineering fields such as high-velocity impact engineering, projectile aerodynamics, creation of new materials, etc, since it can create an extremely high-pressure state in very short time. Of many different types of ballistic ranges developed to date, two-stage light gas gun is being employed most extensively. In the present study, a theoretical work has been made to develop a new type of ballistic range which can easily simulate a flying projectile. The present ballistic range consists of high-pressure tube, piston, pump tube, shock tube and launch tube. The effect of adding a shock tube in between the pump tube and launch tube is investigated. This improvement is identified as the reduction in pressures in the high pressure tube and pump tube while maintaining the projectile velocity. Equations of motions of piston and projectile are solved using Runge-Kutta methods. Dependence of projectile velocity on various design factors such as high pressure tube pressure, piston mass, projectile mass, area ratio of pump tube to launch tube and type of driver gas in the pump tube are also analyzed. Effect of various gas combinations is also investigated. Calculations show that projectile velocities of the order 8 km/sec could be achieved with the present ballistic range.

Key Words: Ballistic Range, Two-Stage Light Gas Gun, Projectile Aerodynamics, Launch Tube, Unsteady Flow

Nomenclature

AR : Area ratio of pump tube to launch tube
a : Sound speed
DPR: Diaphragm pressure ratio
d : Diameter
g : Equivalence factor
l : Length
m : Mass
M : Mach number
P : Pressure
T : Temperature
t : Time
u : Velocity
x : Distance

Greek letters

χ : Non-dimensional distance of projectile

* Corresponding Author,
E-mail : kimhd@andong.ac.kr
TEL : +82-54-820-5622; **FAX** : +82-54-823-5495
School of Mechanical Engineering, Andong National University, 388, Songcheon-dong, Andong, Gyeongbuk 760-749, Korea. (Manuscript **Received** July 4, 2005; **Revised** April 10, 2006)

ϕ : Non-dimensional velocity of piston
γ : Ratio of specific heats
λ : Compression ratio
Π : Pressure ratio across shock wave
τ : Non-dimensional time for piston motion
ζ : Non-dimensional distance of piston
ψ : Non-dimensional velocity of projectile
ζ : Non-dimensional time for projectile motion

Sub-scripts

0 : High pressure tube or initial condition
b : Projectile base
d : Pump tube (driver) conditions
e : Pump tube exit conditions
l : Launch tube
max : Maximum
p : Piston
pr : Projectile
ref : Reflected shock wave
s : Shock wave
1 : Before shock
2 : After shock

1. Introduction

The ballistic range is a fluid dynamic device which can accelerate a projectile to high supersonic or hypersonic speeds. Unlike supersonic or hypersonic wind tunnel in which the model under aerodynamic test is fixed at the test section, a projectile in ballistic range is accelerated to very high speeds through a shock compression. Ballistic range has extensively been used in hypervelocity impact engineering, supersonic and hypersonic projectile aerodynamics. Recently much interest has been concentrated on creating an extremely high-pressure state over several tens to hundreds thousand atmosphere using such a ballistic range (Chhabildas et al., 1995 ; Timothy and Lalit, 1995). In this case, the projectile speed has been known to be more than ten kilometers per second.

In general, the conventional ballistic range (Charters, 1987 ; 1995) consists of three tubes, two diaphragms, a piston and a projectile, as schematically shown in Fig. 1. A high-pressure tube

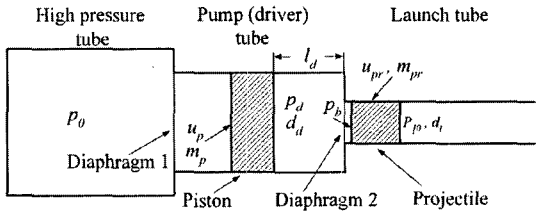

Fig. 1 Schematic of ballistic range

serves as the reservoir of high-pressure gas. Usually, this high-pressure is generated in the tube by firing an explosive. The pump tube, which contains a light-gas, such as helium or hydrogen to rapidly increase the pressure and temperature at the end of isentropic compression process and hence the speed of sound, is connected to the high-pressure tube through a diaphragm separating both at the junction. A massive piston is placed near to the diaphragm in the pump tube.

Projectile is kept in the launch tube which is connected to the pump tube through another diaphragm. Rupture of the diaphragm between the high-pressure tube and pump tube causes the piston to move at a high speed and isentropically compress the light-gas to a much higher pressure than that in the high-pressure tube. With this rapid rise of the pressure inside the pump tube, a state is reached at which the second diaphragm ruptures and shock tube flow is initiated with the production of a strong unsteady shock wave in the launch tube. Resulting high-pressure state just behind the projectile is produced by the reflection of the shock wave from the projectile base, driving the projectile with a very high velocity.

The ballistic range is often called "a two-stage light gas gun". This is not because the ballistic range has two-diaphragms, but the projectile attains energy in two stages. Energy of the high-pressure gas is first transferred to the light-gas in the pump tube through an isentropic compression process and then to the projectile through an unsteady shock wave. In general, the performance of the ballistic range can be determined by the projectile speed at a given pressure in the high-pressure tube and a given mass of the piston. In this case, the projectile speed is also dependent on many other parameters such as, the kind of

light gas (driver gas), length and area of each tube, isentropic compression process of the piston and the shock compression just behind the projectile.

Until now, a large number of pioneering works have been carried out to design the ballistic range and assess its performance (Doolan, 2001 ; Lewis, 1990 ; Tani et al., 1994 ; Bogdonoff, 1997). It has been known that the best performance of the ballistic range would occur when the projectile base pressure due to the shock wave could be kept constant so that the projectile could have a constant acceleration in the launch tube. This is, in part, because there is a limit in accelerating the projectile without giving rise to material strength problem, in which the failure of the projectile can occur at very high acceleration rates.

Smith (1963) and Lukasiewics (1967) have reported the performance of the ballistic range having a constant acceleration. Stalker (1964 ; 1967) and Glass & Sislian (1994) have investigated the effect of the tube area on the shock wave strength and the performance of shock tunnels and ballistic range. Bogdanoff & Miller (1995) have reported the effect of adding a diaphragm in the pump tube. According to their results, with the addition of the diaphragm, the performance of the ballistic range is improved due to the reduction of both the maximum pressures in the pump tube and at the projectile base, while maintaining the same projectile velocity. Recently, Doolan & Morgan (1999) have made a theoretical analysis to design the cost-effective ballistic range, and have suggested a new two-stage free piston driver with a unique compound piston design. Although many other works have contributed to the performance improvement of the ballistic range to date, the complete design of the ballistic range still demands the solutions of many intricate issues with regard to modeling the unsteady processes that can have vital roles to play in the actual implementation stage.

The objective of the present study is to develop a new type of ballistic range which can easily simulate the aeroballistics and impact dynamics in the hyper-velocity regime. A theoretical analysis has been carried out to determine the major design parameters such as the pressure in the high-pressure tube, the masses of the piston and projectile, the kind of light-gas, the area of each tube, etc. A shock tube is added in between the pump tube and the launch tube since it can facilitate to control the projectile speed and/or to mount the projectile in the launch tube. One-dimensional, unsteady, compressible equations have been used to describe the motions of piston and projectile and the resulting equations are solved using 5-stage Runge-Kutta method, with several assumptions of no viscous and heat transfer effects. The present inviscid analytical results show that for the projectile having mass ranging from 5 g to 50 g, projectile speed of the order of 5 km/s to 8 km/s could be achieved.

2. Analytical Study

2.1 Methodology

The schematic and nomenclature of the ballistic range at various sections are shown in Fig. 1. Immediately after the rupture of high pressure tube diaphragm, the piston is driven by the high pressure gas. Motion of the piston is implicitly decided by the difference of pressures on both sides of it, the pressure in front of the piston being isentropic compression pressure on the driver gas. In order to find out the pressure acting at the rear side of the piston during its motion, it is assumed that the high pressure tube acts as a large reservoir of air such that the pressure in the high pressure tube is constant during the complete action of ballistic range, and that any perturbation at the rear side of the piston is subjected to a simple wave traveling through still air (Rudinger, 1955). Whenever, in the calculations, a characteristic terminates at the piston, the required boundary condition is then given by the piston velocity at that instant. The pressure acting on the front side of the piston can be found out from the isentropic relations. While modeling the motion of the piston, driver gas inertia is neglected with dissipation effects caused by the flow between the piston and the pump tube. Moreover, the piston is assumed to move without friction and seal perfectly against the wall.

The projectile is driven by unsteady shock wave generated due to the rupture of pump tube diaphragm. The pressure acting at the base of the projectile can be found out using unsteady gas dynamic equations in a tube with sudden area reduction at the diaphragm junction (Glass and Sislian, 1994), with the assumption that no reflected rarefaction wave from the piston overtakes the base of the projectile. The driving pressure on the projectile can thus be calculated as the difference between projectile base pressure due to shock compression and the initial launch tube pressure acting in front of the projectile. Equation of motion of projectile can be solved as in the case of the piston.

2.2 Formulation

2.2.1 Piston motion

As schematically illustrated in Fig. 1, the pressure acting at the rear side of the piston can be found out as follows.

Defining the non-dimensional quantities,

$$\bar{u}=\frac{u_p}{a_0},\ \bar{a}=\frac{a}{a_0} \tag{1}$$

where, u_p, a_0 and a are the piston velocity, initial sound speed in the high pressure tube and sound speed during the piston motion, respectively.

The piston is assumed to be accelerating from an initial state where the pressure is equal to that in the high pressure tube and the velocity is zero. Several characteristics of expansion waves are created by the motion of the piston. The first characteristic generated due to the piston motion is a Q wave which moves with a velocity

$$\bar{u}-\bar{a}=\bar{a}_0=1,$$
$$(\bar{u}=0 \text{ at initial conditions, } \bar{a}_0=1)$$

Following points of the piston are all characterized by constant P characteristics due to the absence of the right running waves toward the left side of the piston. During the piston motion, a Q wave travels with a velocity of $\bar{u}_{pA}-\bar{a}_A$, where $\bar{u}_{pA}$ is the velocity of piston at a certain point A. P characteristic at the rear side of the piston at initial conditions is given by

$$\frac{2}{\gamma_0-1}\bar{a}_0+\bar{u}_0 \tag{2}$$

The P characteristic through the point A during piston motion is given by

$$\frac{2}{\gamma_0-1}\bar{a}_A+\bar{u}_{pA} \tag{3}$$

Since at the rear side of the piston, the P characteristics are constant as no compression waves travel upstream, hence

$$\frac{2}{\gamma_0-1}\bar{a}_A+\bar{u}_{pA}=\frac{2}{\gamma_0-1}\bar{a}_0+\bar{u}_0 \tag{4}$$

Using isentropic relations,

$$\frac{2}{\gamma_0-1}\left(\frac{p_A}{p_0}\right)^{\frac{\gamma_0-1}{2\gamma_0}}=\frac{2}{\gamma_0-1}-\frac{u_{pA}}{a_0} \tag{5}$$

Then, the pressure acting on the rear side of the piston at any time is given as,

$$p=p_0\left(1-\frac{u_p}{a_0}\left(\frac{\gamma_0-1}{2}\right)\right)^{\frac{2\gamma_0}{\gamma_0-1}} \tag{6}$$

On the front side of piston, the driver gas is being compressed isentropically. Using isentropic relations,

$$\frac{p_d}{p_{d_0}}=\left(\frac{x}{l_d}\right)^{-\gamma_d}=\lambda^{-\gamma_d} \tag{7}$$

where, λ is the compression ratio, defined as the ratio of initial gas volume in the pump tube to the gas volume at diaphragm rupture.

Equation of motion of the piston reduces to

$$-m_p\left(\frac{d^2x}{dt_p^2}\right)$$
$$=\frac{\pi.d_d^2}{4}\left(p_{d_0}\lambda^{-\gamma_d}-p_0\left(1-\frac{u_p}{a_0}\left(\frac{\gamma_0-1}{2}\right)\right)^{\frac{2\gamma_0}{\gamma_0-1}}\right) \tag{8}$$

Introducing dimensionless variables,

$$\xi(\tau)=\frac{x}{d_d},\ \tau=\frac{t_p.a_0}{d_d},\ \phi(\tau)=\frac{u_p}{a_0} \tag{9}$$

Using the dimensionless parameters, Eq. (8) along with initial conditions can be written as,

$$\dot{\xi}=-\phi$$
$$\dot{\phi}=-c_1\left(c_2\xi^{-\gamma_d}-\left(1-\frac{\gamma_0-1}{2}\right)^{\frac{2\gamma_0}{\gamma_0-1}}\right) \tag{10}$$
$$\xi(0)=\frac{l_d}{d_d},\ \phi(0)=0$$

where, dots denote differentiation with respect to τ and the constants c_1 and c_2 are given by

$$c_1=\frac{\pi}{4}\frac{p_0.d_d^3}{m_p.a_0^2}$$
$$c_2=\frac{p_{d_0}}{p_0}\left(\frac{l_d}{d_d}\right)^{\gamma_d} \quad (11)$$

Eq. (10) is solved using Runge-Kutta method which has 5th order accuracy.

2.2.2 Projectile motion

Equation of motion of projectile is modeled with the use of unsteady shock wave generated due to diaphragm rupture.

Equation of motion of projectile can be given as,

$$m_{pr}\frac{d^2x}{dt_{pr}^2}=\frac{\pi d_t^2}{4}(p_b-p_{t_0}) \quad (12)$$

where, p_b is the shock compression pressure at the base of the projectile.

For a tube with area change, the pressure due to diaphragm rupture is given by (Glass and Sislian, 1994),

$$\frac{p_b}{p_r}=g\left[1-g^{-\left(\frac{\gamma_d-1}{2\gamma_d}\right)}\right]^{\frac{2\gamma_d}{\gamma_d-1}} \quad (13)$$

where, u_{pr} is the projectile velocity due to gas mass motion behind the unsteady shock, and g is the equivalence factor based on the ratio of area of pump tube to launch tube, which is given by the Mach number of unsteady expansion waves traveling into the pump tube.

$$g=\left[\frac{\gamma_d+1\,(2+(\gamma_d-1)\,M_e^2)}{(2+(\gamma_d-1)\,M_e)^2}\right]^{\frac{\gamma_d}{\gamma_d-1}} \quad (14)$$

Assuming choked flow at the diaphragm section immediately after the diaphragm rupture, M_e can be found out from the isentropic relations as

$$\frac{d_d^2}{d_t^2}=AR=\frac{1}{M_e^2}\left[\frac{2}{\gamma_d+1}\left(1+\frac{\gamma_d-1}{2}M_e^2\right)\right]^{\frac{\gamma_d+1}{\gamma_d-1}} \quad (15)$$

With the dimensionless parameters

$$\chi=\frac{\pi d_t^2}{4}\frac{p_r}{m_{pr}a_r^2}x$$
$$\zeta=\frac{m d_t^2}{4}\frac{p_r}{m_{pr}a_r}t_{pr},\ \psi=\frac{u_{pr}}{a_r} \quad (16)$$

using Eqs. (13) & (14), Eq. (12) with the initial conditions becomes

$$\frac{d^2\chi}{d\zeta^2}=g\left[1-g^{-\left(\frac{\gamma_d-1}{2\gamma_d}\right)}\frac{\gamma_d-1}{2}\psi\right]^{\frac{2\gamma_d}{\gamma_d-1}}-\frac{1}{DPR} \quad (17)$$
$$\chi(0)=0,\ \dot{\chi}(0)=0$$

where, p_r, and a_r are the pressure and speed of sound at diaphragm rupture, respectively, and DPR is the diaphragm pressure ratio, defined as p_r/p_{t0}. During the above formulation, it is assumed that no expansion waves which are produced due to the reflection of the shock wave on the shock tube or pump tube end and piston, reach the base of the projectile, leading to reduction in the effective acceleration of the projectile.

2.2.3 Shock tube in between pump tube and launch tube

The schematic of ballistic range with shock tube is shown in Fig. 2. Projectile is accelerated in launch tube due to the double compression of gases using piston and unsteady shock wave. Owing to large pressure ratio needed to produce a strong unsteady shock in launch tube, initial high pressure tube pressure required to drive the piston for isentropic compression of driver gas should be quite large. The technique of adding a shock tube or additional diaphragm in pump tube would provide the required high pressure ratio across launch tube diaphragm as reported by Bogdanoff and Miller (1995). Then, effective work done by the piston can be reduced as pressure needed to break the shock tube diaphragm could be much less than that needed to break launch tube diaphragm, on which high pressure is produced due to the shock wave reflection. Small amount of work done during the rupture of the diaphragm can be neglected. This not only saves the high pressure tube

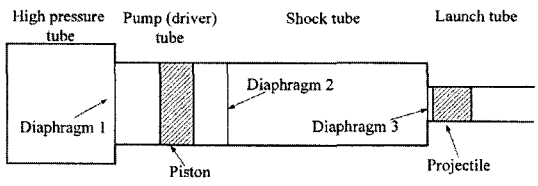

Fig. 2 Schematic of ballistic range with shock tube

pressure, but increases the sound speed and velocity of gas entering the launch tube due to the high temperature produced by the shock reflection.

A normal shock wave is produced in the shock tube after the pump tube diaphragm rupture. This shock wave travels into the shock tube, and at the same time, an expansion wave travels into the pump tube. Using the characteristic relations of P and Q waves, the gas velocity behind the shock wave can be written as

$$\frac{u_m}{a_{r_s}}=\frac{2}{\gamma_d-1}\left[1-\left(\frac{p_2}{p_{r_s}}\right)^{\frac{\gamma_d-1}{2\gamma_d}}\right] \tag{18}$$

where, u_m is the gas velocity behind the normal shock wave, a_{r_s} and p_{r_s} are thesound speed and pump tube pressure at shock tube diaphragm rupture, respectively.

The gas velocity behind the normal shock wave is given by the normal shock relations,

$$\frac{u_m}{a_{s_0}}=\left(\frac{p_2}{p_1}-1\right)\left[\frac{2}{\gamma_s\left((\gamma_s+1)\frac{p_2}{p_1}+(\gamma_s-1)\right)}\right]^{\frac{1}{2}} \tag{19}$$

where, a_{s_0} is the initial sound speed in the shock tube.

Elimination of the gas velocity in Eqs. (18) & (19) yields

$$\frac{p_{s_0}}{p_{r_s}}=\frac{1}{\Pi_{21}}\left[1-(\Pi_{21}-1)\left(\frac{\gamma_d-1}{2\gamma_d}\left(\frac{K\frac{T_{s_0}}{T_{r_s}}}{\frac{\gamma_s+1}{\gamma_s-1}\Pi_{21}+1}\right)^{\frac{1}{2}}\right)^{\frac{2\gamma_d}{\gamma_d-1}}\right] \tag{20}$$

where, $\Pi_{21}=p_2/p_1$ is the pressure ratio across the shock wave, K is the ratio of specific heats of pump tube and shock tube gases at constant volume and p_{s0}/p_{rc} is the pressure ratio across the pump tube-shock tube diaphragm.

The shock Mach number is given by

$$M_s=\left[\frac{(\gamma_s-1)}{2\gamma_s}\left(1+\frac{\gamma_s+1}{\gamma_s-1}\Pi_{21}\right)\right]^{\frac{1}{2}} \tag{21}$$

For the reflected shock,

$$\Pi_{ref}=\frac{p_{ref}}{p_2}=\frac{\frac{\gamma_s+1}{\gamma_s-1}+2-\Pi_{21}}{1+\frac{\gamma_s+1}{\gamma_s-1}\Pi_{21}} \tag{22}$$

From Eq. (22), pressure on the shock tube-launch tube diaphragm after shock wave reflection could be determined.

4. Results & Discussion

The pump tube pressure history for different piston masses is presented in Fig. 3, where conventional ballistic range without shock tube is considered with a constant pressure of 5 MPa in the high pressure tube. Diaphragm rupture pressure is assumed to be 150 MPa. Diameter and length of pump tube are fixed as 60 mm and 1 m, respectively. During the initial period of piston motion, the pressure and temperature rises in driver gas (helium) are marginal. By far, greater fraction of rise occurs in the very last part of the stroke. It is clear that, the heavier the piston, the more is the time taken to achieve the rupture pressure. It is also observed that with a piston mass of 0.4 kg, the minimum constant pressure in the high pressure tube to obtain the required rupture pressure is 4.51 MPa with a piston speed of 0.99 m/s at rupture. The piston velocity at diaphragm rupture is an important parameter as it decides the momentum with which the piston hits at the end of the pump tube. It is generally termed as the residual piston velocity. If the high pressure tube pressure is below this pressure, piston seizes before it could develop the required rupture pressure of 150 MPa. It is possible to arrange the high pressure tube pressure, piston mass and initial pump tube pressure in such a way to obtain the residual piston velocity as low as possible to avoid piston/pump tube end damage, while all other parameters remain constant. When the length of pump tube is increased to 2 m, the minimum pressure in high pressure tube is raised to 5.72 MPa with a residual piston velocity of 1.253 m/s. Minimum pressure in high pressure tube is decreased to 3.76 MPa with a residual piston velocity of 1.06 m/s, when the diameter of pump tube is decreased to 40 mm, while the length of the pump tube being 1 m. Variations of piston velocity under these conditions is shown in Fig. 4. These data can provide only a rough estimate of the mass and high pressure tube pressure as the

diaphragm rupture pressure is hard to predict accurately. The pressure history in pump tube for various high pressure tube pressures is also shown in Fig. 5 with initial pump tube parameters.

Projectile velocity history is plotted in Fig. 6 for different projectile masses. Projectile achieves very high velocities in short time and the values are highly sensitive to projectile mass. In Fig. 7, the projectile motion is illustrated for various projectile masses. It is worth while noting that a heavier projectile is desirable for the length constraints of the launch tube. Figures 8 and 9 show the dependence of the area ratio of pump tube to launch tube on projectile velocity. It is known that we don't need excessive area ratios to achieve appreciable gain in projectile velocity, as reported by Glass and Sislian (1994). Projectile velocities of various ballistic range geometries are shown in Fig. 10. Also, it is clearly evident that a stepped geometry (Case C) with sudden re-

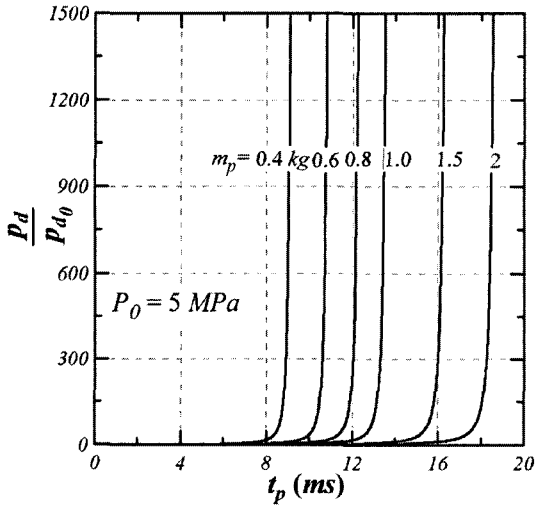

Fig. 3 Pump tube pressure history for various piston masses

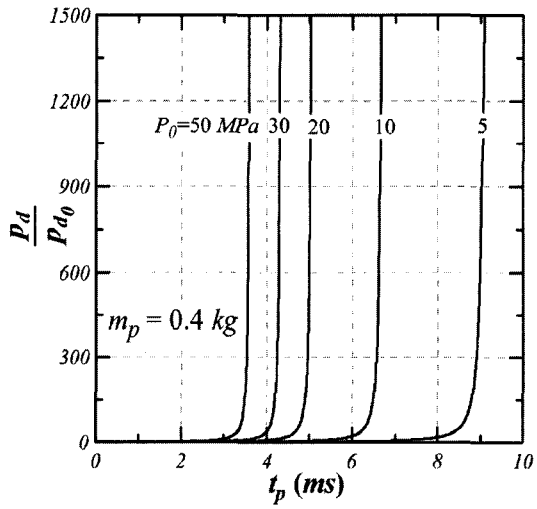

Fig. 5 Pump tube pressure history for various high pressure tube pressures

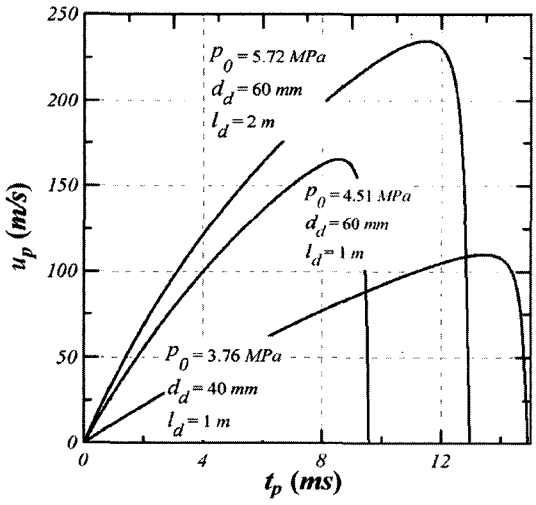

Fig. 4 Piston velocity history at various conditions

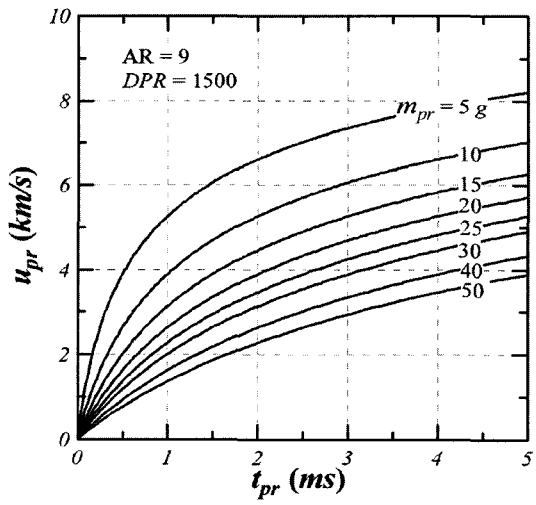

Fig. 6 Projectile velocity history for various projectile masses

ductions in area at the diaphragm sections, yields maximum projectile velocity at all distances. For case A in which the pump tube and shock tube have the same diameters, the projectile velocity is found to be a little higher than that in case B within a launch tube length of 2.5 m. However, beyond this distance, projectile velocity in case B overcomes the projectile velocity in case A.

The operating process of ballistic range is shown in Fig. 11. Peak pressure experienced by the projectile at the base is a major design parameter due to the fact that very high base pressures lead to structural failure of the projectile as pointed out by Doolan (2001) and Glenn (1990). The projectile base pressure history is also shown in Fig. 11.

Addition of shock tube leads to a gain in high pressure tube pressure. Figure 12 shows the operating processes of ballistic range with shock tube. The length of the shock tube is fixed as 2 m in the

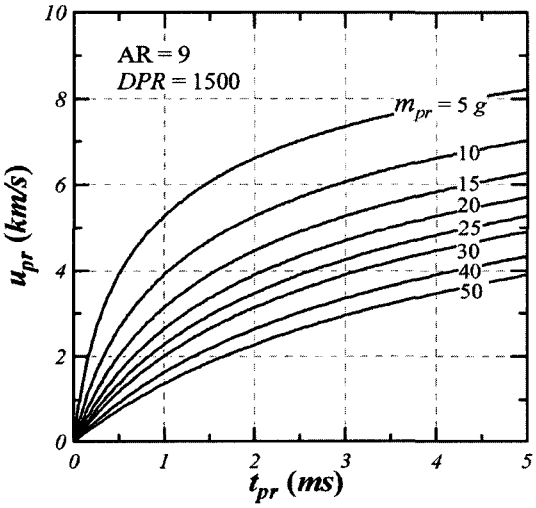

Fig. 7 Projectile locations and velocities for various projectile masses

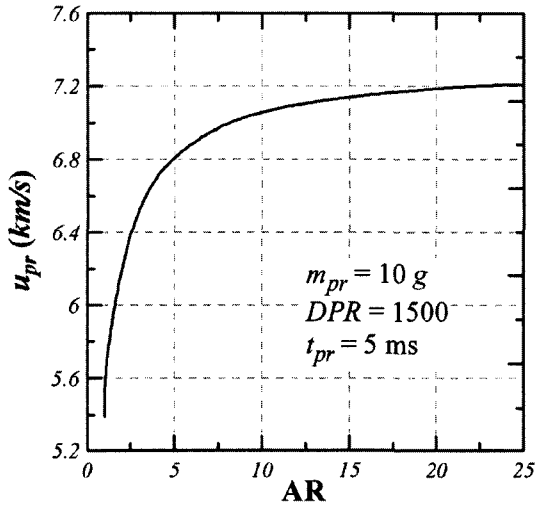

Fig. 9 Variation of projectile velocity with area ratio

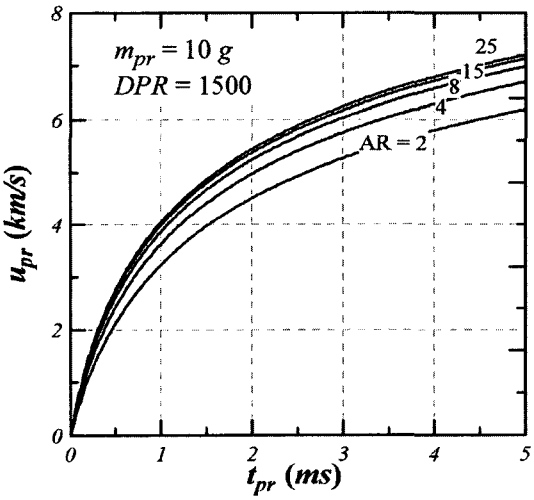

Fig. 8 Projectile velocity history for various area ratios

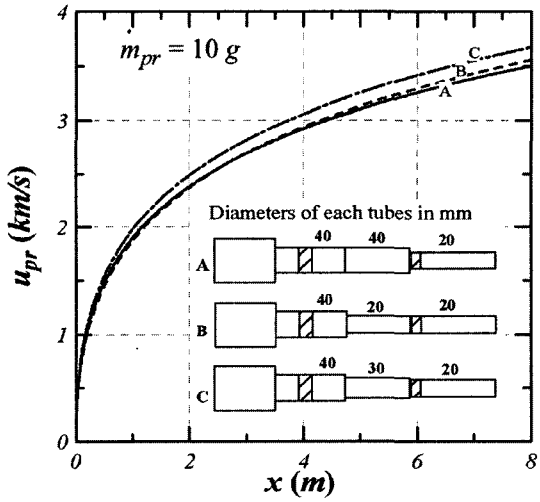

Fig. 10 Projectile velocities in various ballistic range geometries

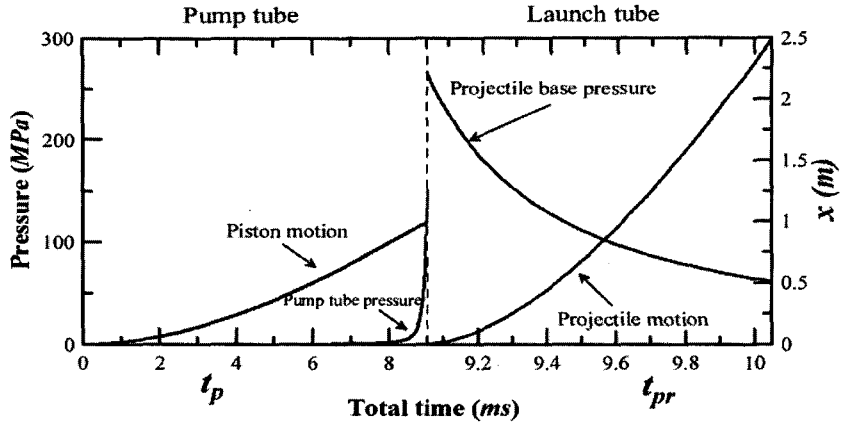

Fig. 11 Operating process of ballistic range

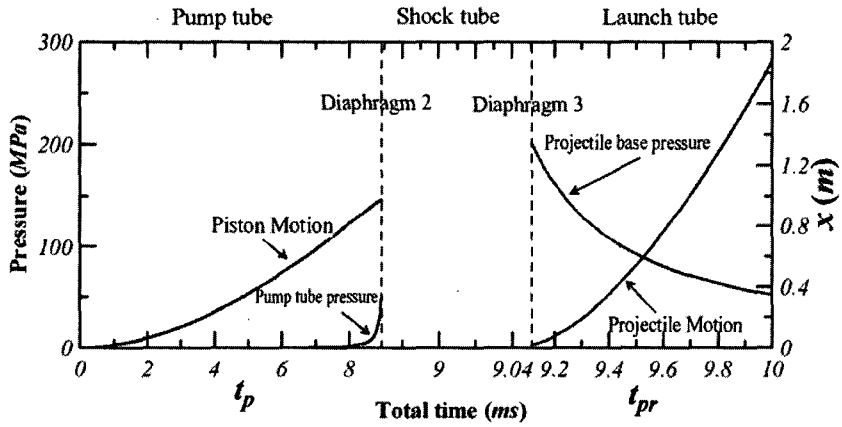

Fig. 12 Operating process of ballistic range with shock tube

analysis. In the present inviscid analysis, addition of shock tube improves system performance in terms of the gain in high pressure tube pressure. Bogdanoff and Miller (1995) reported that in actual case, the gain is marginal due to heat transfer and friction effects at the pump tube wall.

Figure 13 shows the dependence of various gas combinations in pump tube and shock tube on the projectile velocity and maximum base pressure. Table 1 gives the values of maximum pressures in the ballistic range and at the projectile base. Columns with the term "shock" refer to the conditions of unsteady shock wave traveling in the shock tube. With a gas combination hydrogen-argon-air (case E in Table1), projectile achieves a maximum velocity of ~4.6 km/s within 3 ms after the launch tube diaphragm rupture. The maximum pressures at the projectile base and in

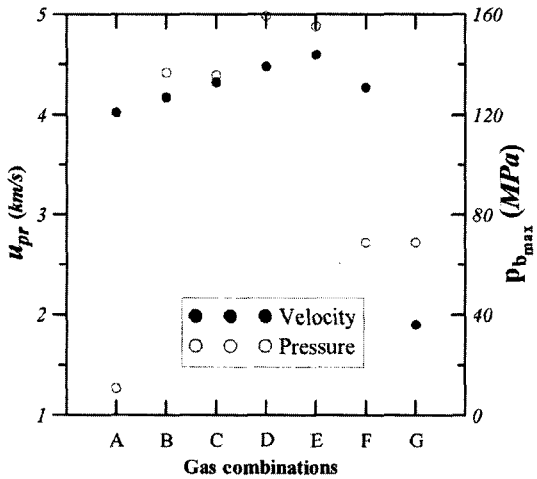

Fig. 13 Effect of various gas combinations on projectile velocity and maximum projectile base pressure

Table 1 Values of projectile velocities and pressures for various gas combinations

	Gas Combinations	u_{pr} (km/s)	p_{bmax} (MPa)	a_r (km/s)	M_s (shock)	p_2/p_1 (shock)	*DPR*
A	Hydrogen-Helium-Air	4.021	48.008	5.509	6.19	47.62	262
B	Helium-Air-Air	4.174	142.603	2.285	9.72	110.16	380
C	Helium-Argon-Air	4.321	141.802	2.896	10.33	133.22	775
D	Hydrogen-Air-Air	4.480	159.613	2.408	10.25	122.65	929
E	Hydrogen-Argon-Air	4.598	156.482	3.036	10.83	146.5	855
F	Helium-Air (without shock tube)	4.272	91.621	3.098	—	—	500
G	Argon-Air (without shock tube)	1.942	91.621	1.115	—	—	500

the shock tube to achieve this speed are about 160 MPa and 85.5 MPa, respectively. These high pressures can lead to projectile failure and reduced system lifetimes. Therefore, improved system performance is interpreted as an increase in projectile velocity while maintaining peak pressures or as a decrease in peak pressures while maintaining projectile velocity. A combination of hydrogen-helium-air (Case A) can be considered to be superior to all other combinations as the maximum pressure in the ballistic range and at the projectile base is much less than that of others with little loss of projectile velocity. Increase in projectile velocity in case E is 14.4% as compared to case A, while the increase in peak pressure is 226%. Case F (without shock tube), when compared with case A, shows an increase of 6.2% in velocity and 90% increase in maximum pressure. It is worth while noting that in case A, with a diaphragm pressure ratio of 500 in the pump tube, the maximum pressure produced in the shock tube is only 26.2 MPa, which is the launch tube diaphragm rupture pressure. Case F, when examined with this diaphragm rupture pressure, could produce a projectile velocity of 3.03 km/s with the same peak pressure at the projectile base. From these data, it is possible to select the suitable gas combination to optimize the system performance in conjunction with other parameters.

The present analysis can be applied to obtain the practical design parameters of the ballistic range. Due to the assumption of inviscid flows, the projectile velocities might be overestimated. Hence studies on dissipation effects can be important to predict the projectile velocities and system performance accurately. Future studies are therefore planed to extend the analysis with addition of friction, heat transfer and leakage effects and to experimentally validate the results.

5. Conclusions

A theoretical analysis is carried out to determine the design parameters of a ballistic range. One-dimensional unsteady compressible equations are solved to obtain the required design parameters of ballistic range. Piston and projectile motions are modeled using unsteady one-dimensional equations. It has been observed in the present analysis that projectile velocities of the order 8 km/sec could be achieved. The calculated projectile velocities are little overestimated due to neglecting the shock as well as expansion waves at the end of the shock tube/pump tube and piston.

The major results are summarized as follows,

(1) Projectile velocities are highly sensitive to projectile mass and the diaphragm pressure ratio, and the piston motion could be optimized by properly arranging piston mass and high pressure tube pressure. This avoids the impact of the piston at the pump tube end with a very high velocity and thereby improves the lifetime of piston and ballistic range components.

(2) Considerable increase in the projectile velocity could be obtained with increased area ratios of pump tube to launch tube. However, area

ratios beyond 20 do not yield extensive gain in projectile velocity. Addition of a shock tube to pump tube saves high pressure tube pressure and time for which it is to be maintained constant during the piston motion. The geometry with sudden reductions in area at both the diaphragm sections leads to enhanced projectile velocities.

(3) With suitable gas combinations in pump tube and shock tube, performance of ballistic range could be improved in terms of peak pressures at projectile base and in the components. A combination of hydrogen-helium-air in the ballistic range is seen to be superior to all other gas combinations in terms of ballistic range performance.

Acknowledgments

This research was supported by the Program for the Training of Graduate Students in Regional Innovation which was conducted by the Ministry of Commerce Industry and Energy of the Korean Government.

References

Bogdanoff, D. W. and Miller, R. J., 1995, "Improving the Performance of Two Stage Light Gas Guns by Adding a Diaphragm in the Pump Tube," *Intl. J. Impact Engineering*, Vol. 17, pp. 81~92.

Bogdonoff, D. W., 1997, "Optimization Study of The Ames 0.5 Two-Stage Light Gas Gun," *Intl. J. Impact Engineering*, Vol. 20, pp. 131~142.

Charters, A. C., 1987, "Development of High-Velocity Gas-Dynamics Gun," *Intl. J. Impact Engineering*, Vol. 5, pp. 183~207.

Charters, A. C., 1995, "The Early Years of Aerodynamic Ranges, Light-Gas Guns, and High Velocity Impact," *Intl. J. Impact Engineering*, Vol. 17, pp. 151~182.

Chhabildas, L. C., Kmetyk, L. N., Reinhart, W. D. and Hall, C. A., 1995, " Enhanced Hypervelocity Launcher — Capabilities to 16 Km/s," *Intl. J. Impact Engineering*, Vol. 17, pp. 183~194.

Doolan, C. J. and Morgan, R. G., 1999, "A Two-Stage Free-Piston Driver," *Shock Waves*, Vol. 9, pp. 239~248.

Doolan, C., 2001, "A Two Stage Light Gas Gun for the Study of High Speed Impact in Propellants," DSTO Report, DSTO-TR-1092.

Glass, I. I. and Sislian, J. P., 1994, "Nonstationary Flows and Shock Waves," *Oxford Science Publications*, Oxford, pp. 100~125.

Lewis, A. G., 1990, "Design Limitations on Ultra-High Velocity Projectile Launchers," *Intl. J. Impact Engineering*, Vol. 10, pp. 185~196.

Lukasiewics, J., 1967, "Constant Acceleration Flows and Applications to High Speed Guns," *J. AIAA*, Vol. 5, No. 11, pp. 1955~1963.

Rudinger, G., 1955, "Wave Diagrams for Nonsteady Flows in Ducts," *D. Van Nostrand Company, Inc.*, pp. 56~59.

Smith, F., 1963, "Theory of Two Stage Hypervelocity Launcher to Give Constant Driving Pressure at the Model," *J. Fluid Mechanics*, Vol. 17, pp. 113~125.

Stalker, R. J., 1964, "Area Change with a Free Piston Shock Tube," *J. AIAA*, Vol. 2, pp. 396~397.

Stalker, R. J., 1967, "A Study of Free Piston Shock Tunnel," *J. AIAA*, Vol. 5, pp. 2160~2165.

Tani, K., Itoh, K., Takahashi, M., Tanno, H., Komuro, T. and Miyajima, H., 1994, "Numerical Study of the Free-Piston Shock Tunnel Performance," *Shock Waves*, Vol. 3, pp. 313~319.

Timothy, G. T. and Lalit, C. C., 1995, "Computational Design of Hypervelocity Launchers," *Intl. J. Impact Engineering*, Vol. 17, pp. 849~860.